Materials Research. 2023; 26:e20230214
DOI: https://doi.org/10.1590/1980-5373-MR-2023-0214

Influence of Hot Rolling on β Ti-Nb-Zr(-Ta) Multiprincipal Alloys for Biomedical Application

Rafael Formenton Macedo dos Santos [a], ***Pedro Akira Bazaglia Kuroda*** [b]*, ***Carolina Neves Reis*** [b], ***Conrado Ramos Moreira Afonso*** [b]

[a]*Universidade Federal de São Carlos (UFSCar), Programa de Pós-Graduação em Ciência e Engenharia de Materiais (PPG-CEM), 13565-905, São Carlos, SP, Brasil*
[b]*Universidade Federal de São Carlos (UFSCar), Departamento de Engenharia de Materiais (DEMa), 13565-905, São Carlos, SP, Brasil.*

Received: April 19, 2023; Revised: August 01, 2023; Accepted: September 01, 2023

With increasing life expectancy, revision surgeries have become more frequent in implanted people. This is due to the biological and biomechanical incompatibility that generates, among others, problems such as *stress shielding*. This works aims to analyze the influence of the hot rolling process (HR sample) on the microstructure and, consequently, the properties of β-Ti multiprincipal alloys: Ti-27Nb-39Zr (39Zr), Ti-30Nb-50Zr (50Zr), and Ti-20Nb-30Zr-13Ta (30Zr) (wt. %.) (equimassic and with high content of β-stabilizer elements). All samples were subjected to characterization through X-ray diffraction (XRD) to determine the phases present, and optical microscopy (OM) and scanning electronic microscopy (SEM) were realized to characterize the microstructure and confirm the phases obtained through XRD. Before hot rolling, only the β phase was identified, but in the HR condition, the α and β phases were identified. Consequently, it did not observe significant changes in microhardness for all alloys, while the elastic modulus was observed with a reduction of 23% for 39Zr, 46% for 40Zr, and 13% for 30Zr. The hot rolling processing was confirmed to be a helpful route to reduce the elastic modulus for β Ti multiprincipal alloys opening perspectives for applying such alloys as metallic implant materials.

Keywords: *β-Ti alloys; Multiprincipal Alloys, Microstructure Characterization; Hot Rolling.*

1. Introduction

With the increase in life expectancy, revision surgeries have become more frequent in implanted people[1-3]. Among the main reasons that contribute to this increase, it can mention two meaningful problems: the biological incompatibility, the presence of chemical elements such as Al, in Ti-6Al4-V (110 GPa) alloy, and Ni, in stainless steels ASTM F138 (200 GPa), can cause health problems such as Alzheimer's disease and cancer, respectively[4-8], the biomechanical incompatibility, when elastic modulus value of the implant material is much higher than that of the bone, leading the phenomenon known as stress shielding[4]. The stress-shielding effect is associated with bone resorption in the region of contact between the bone and the implant, can generate bone weakening and inadequate implant fixation, and may even cause the implant to loosen[9-11].

In this scenario, β-titanium alloys (β-Ti) with low elastic modulus and free of toxic elements in their chemical composition[12,13], like niobium (Nb), zirconium (Zr), and tantalum (Ta), have been developed for application as biomaterials, considering that β-Ti alloys present good corrosion resistance and better biological and mechanical compatibility when compared to the commercial alloys currently used[14-20].

The phase composition of β-Ti alloys is determined by the presence and content of β-stabilizing elements, as well as processing routes, including cooling rate imposed, heat treatments, and thermomechanical treatments[19,21-26]. Among the phases that can be formed, the ω phase has the highest elastic modulus and the highest hardness, and the α″ phase (orthorhombic) has the lowest elastic modulus and hardness[27,28]. It is essential to highlight that the martensitic α″ phase can be formed both via stress-induced martensite (SIM), the deformation-induced transformation of the β-phase, as well as by rapid quenching from the β field[28-30].

Thermomechanical processes are widely used to obtain semi-finished products and to adjust some mechanical properties of metallic materials[31-35]. Among these processes, it can mention cold, hot rolling, and rotary swaging. While hot rolling produces longitudinal deformation in the metallic material, hot swaging, or rotary forging, promotes radial deformation through the sample. These processes apply plastic deformation in order to shape the metallic materials and promote recrystallization, texture, and/or phase transformation, which influences these materials' properties[31-35]. In the case of β-Ti alloys, plastic deformation induces the phase transformation from β to α″ phase (SIM), which in turn leads to a decrease in the values of the elastic modulus, and therefore is a crucial processing route for the optimization of β titanium alloys[32-35].

*e-mail: pedro@fc.unesp.br

Senopatti and Sutowono (2023) analyze the effect of the hot rolling process (900, 1000, and 1100 °C) on the structure and hardness of α/β Ti-6Al-6Nb alloy for orthopedic application. The study revealed that hot rolling at 1000 °C has the lowest hardness, and rolling at 900 °C has the highest hardness value. The finer grain size increases the hardness value of hot-rolled Ti-6Al-6Nb[36].

This work aims to analyze the influence of the hot rolling process (thermomechanical) on the microstructure and, consequently, mechanical properties of multiprincipal β-Ti alloys in different compositions and the number of alloying elements: Ti-27Nb-39Zr (39Zr), Ti-30Nb-50Zr (50Zr), and Ti-20Nb-30Zr-13Ta (30Zr) (wt. %.) β-Ti alloys (equimassic and with high content of β-stabilizer elements).

The 30Zr, 39Zr, and 50Zr alloys form part of a new group of β-Ti alloys yet to be studied. According to the Mo equivalent theory (Mo_{eq} = Nb*0.28 + Ta*0.22 +Zr*0.11), the 30Zr, 39Zr, and 50Zr alloys are of the β-metastable type with Mo_{eq} values corresponding to 11.8, 11.9, and 13.9, respectively[37].

2. Experimental Procedure

From high purity elements (> 99%), 100 g ingots of Ti-27Nb-39Zr (39Zr), Ti-30Nb-50Zr (50Zr), and Ti-20Nb-30Zr-13Ta (30Zr) all in weight percent (wt. %) β-Ti alloys (equimassic and with high content of β-stabilizer elements) were cast through an arc melting furnace, Edmund Bulher model D-72411, under argon protective atmosphere and cooled in a copper mold, named here as the as-cast condition (AC). Subsequently, the ingots were subjected to a heat treatment of solubilization for 15 minutes at a temperature of 1273 K to stabilize the temperature within the β (bcc) phase field. After that, the hot rolling process was started through a conventional (symmetrical) mill, FENN brand, model 051-51019 located at DEMa/UFSCar. The reduction in the thickness per pass was 0.42 mm, and every three passes the samples were reheated at 1273 K for 5 minutes. This process was repeated until an area reduction of approximately 50%. These samples are named here as hot rolled conditions (HR).

To calculate the percentage of reduction in area (%RA), that is, the degree of plastic deformation of the samples, the following equation was used (Equation 1):

$$\%RA = \left(\frac{A_o - A_f}{A_o} \right) x100 \quad (1)$$

where A_o is the initial cross-sectional area, and A_f is the final cross-sectional area[38].

All samples were subjected to metallographic preparation using SiC sandpaper and water as a lubricant, from 240 to 2000 mesh, and then polished 1 μm alumina (Al_2O_3) polished. Finally, chemical etching using a modified Kroll (40% H_2O + 40% HF + 20% HNO_3) aqueous solution by volume revealed the microstructure. To determine the phases present in the samples, was used X-ray diffraction (XRD) via Rigaku Gierflez model by Cu-Kα radiation (λ = 1.54 Å), with a sweep between the angles of 20 - 90°, and with a step size of 2° /min. From the analysis of the XRD, and by manipulating the interplanar distance equations (Equation 2) for cubic systems and Bragg's law (Equation 3), it is possible to determine the lattice parameter, an (Equation 4), as shown below:

$$n\lambda = 2d_{hkl}\text{sen}\theta \quad (2)$$

$$d_{hkl} = \frac{a}{\sqrt{h^2 + k^2 + l^2}} \quad (3)$$

$$a = \frac{n\lambda\sqrt{h^2 + k^2 + l^2}}{2\text{sen}\theta} \quad (4)$$

where n is the order of reflection, λ is wavelength (Å), θ is angle of incidence, *h, k* and *l* are Miller indices, d_{hkl} is interplanar spacing (angstrom), and *a* (Å) is the lattice parameter[38].

Microscopy techniques were used to confirm the phases determined by XRD and determine the grain size and geometry. Optical microscopy (OM) was performed using an Olympus optical microscope, model BX41M-LED, with an Infinity Capture acquisition and processing system. Scanning electron microscopy (SEM) was performed using the Philips XL30 FEG in SE and BSE modes. Furthermore, the SEM-FEG is equipped and coupled to EDS (energy dispersive spectroscopy) EDAX detector system, in order to determine the semi-quantitative chemical composition of the multiprincipal β-Ti alloys.

The elastic modulus, E (GPa) measurements were performed using the Sonelastic equipment from the ATCP company, based on the impulse excitation technique, following the ASTM E1876:2001 standard[39]. Finally, the Vickers microhardness was measured, following the ASTM-E384 standard, using a Shimadzu HMV - G20ST microhardness tester, applying a load of 0.5 kgf for 15 seconds[40].

3. Results and Discussion

The microstructural analysis was based on XRD analysis and microscopy tests to determine the phases present, shape and grain size. Figure 1 shows the XRD patterns and crystallographic planes corresponding to each phase, β-Ti (bcc) and α″ martensite (orthorrombic). For all samples in the as-cast (AC) condition, the presence of only the β-Ti phase was identified. Due to the high content of β-stabilizing elements (elements which stabilize the β-Ti phase), and the cooling rate imposed from the arc melting process in a water-cooled copper hearth crucible, which is not high enough for martensite α" formation. However, when analyzing the diffractograms of the hot-rolled (HR) samples condition, besides identifying the β-Ti phase, it is also possible to identify the martensite α" phase. Such phase formation, as discussed previously, is the result of the plastic deformation to which the alloys were subjected during the rolling process. Thus, the martensite α" phase was formed induced by deformation, so it is stress-induced martensite (SIM). This result is in agreement with the literature[32,33], and it happens even for multiprincipal β-Ti alloys with high content of β-stabilizer elements).

As regular XRD can only detect the presence of phases with a volumetric fraction above 5%, the presence of the omega phase is usually not confirmed by this technique; however, based on the literature, it is likely to be present[35].

To confirm this possibility, it is necessary to use other techniques, such as high-energy XRD or transmission electron microscopy (TEM)[33,41,42]. Through Equation 4 and the crystallographic planes of the β (BCC) phase, it was possible to determine the lattice parameter of this phase, and the same alloy, for both conditions (BC), AC and HR. The values were the same as shown then: a_{50Zr} = 3.4271, a_{39Zr} = 3.3357, and a_{30Zr} = 3.3152 Å, with a clear tendency of increasing of β-Ti phase lattice parameter.

Figure 2 shows the micrographs for all alloys under all conditions. Through it, it is possible to observe that for the AC condition, the microstructure is dendritic (MO), not being possible to determine the grain size. After the hot rolling process, the microstructure changed from the raw melt structure to equiaxial grains (SEM using backscattered electrons, BSE, signal), slightly deformed in the rolling direction and the average grain size (GS) for the alloys, in this condition (HR) are shown followed: GS_{50Zr} = 119, GS_{39Zr} = 102 and GS_{30Zr} = 96 µm. Still, in Figure 2, it is possible to observe equiaxial grains of the β phase with the presence of the acicular phase α" (SIM) in its interior, thus confirming the analyses carried out through the XRD.

Table 1 shows the results for the alloys studied in this work of the semi-quantitative analysis performed using SEM-EDS. This analysis showed that the experimental composition for the 50Zr, 30Zr, and 39Zr alloys is according to plan since a discrepancy of approximately 2% is acceptable, considering that it is a semi-quantitative analysis.

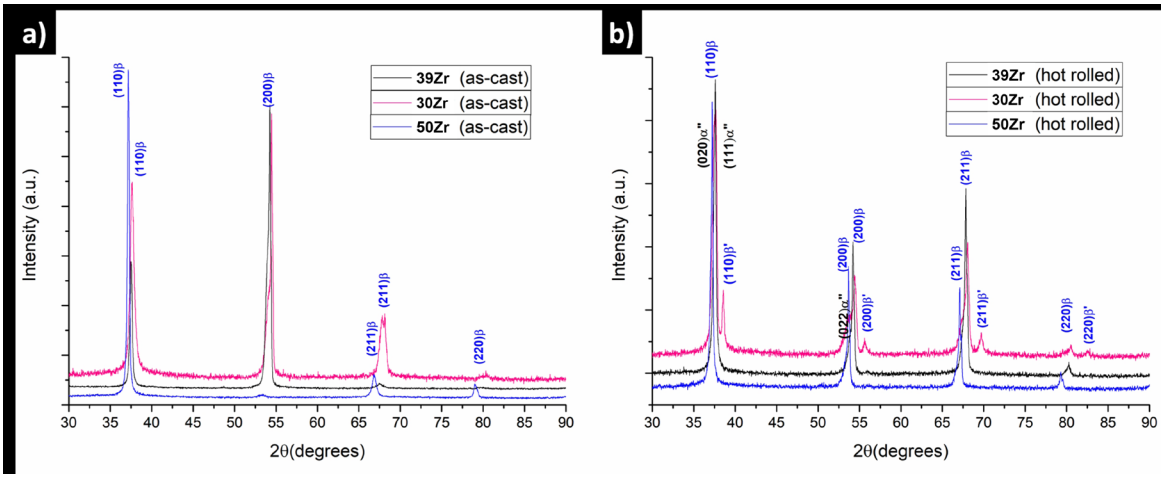

Figure 1. X-ray diffraction (XRD) patterns for β Ti-Nb-Zr(-Ta) alloys in the a) as-cast (AC) and b) hot rolled (HR) conditions.

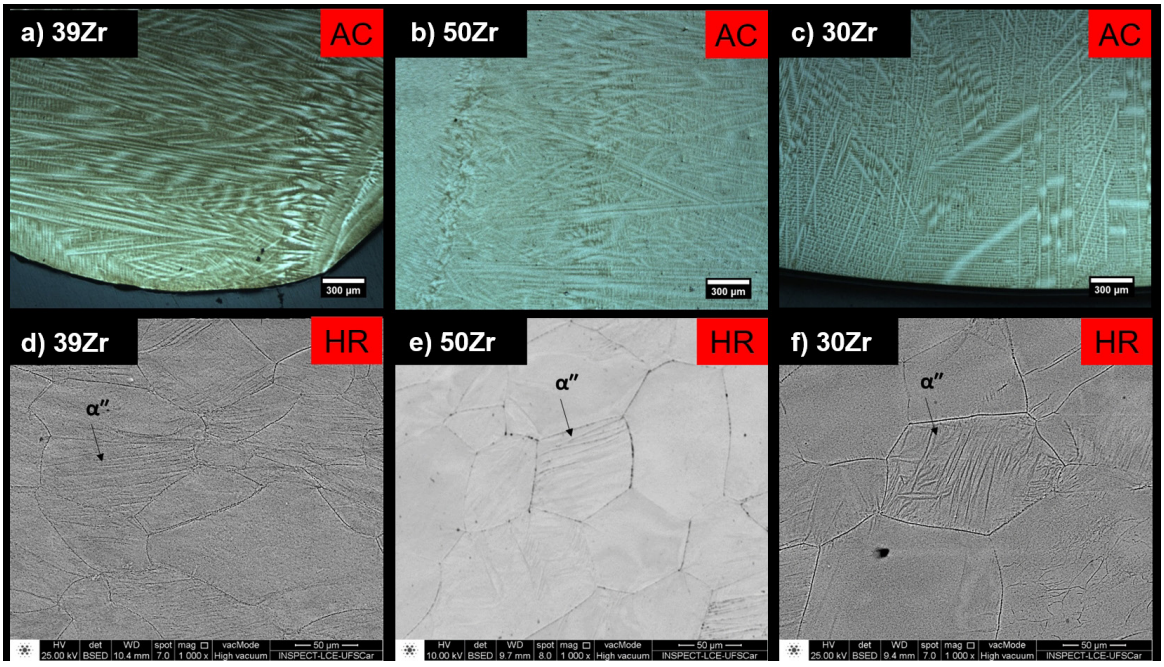

Figure 2. OM images for AC condition and SEM-BSE images for HR condition, respectively, a) and d) 27Zr, b) and e) 50Zr and c) and f) 30Zr.

Table 1. Semi-quantitative chemical composition obtained through SEM-EDS (wt. %) for β Ti-Nb-Zr(-Ta) multiprincipal alloys.

Sample	Nb (wt. %)	Zr (wt. %)	Ta (wt. %)	Ti (%p)
Ti-30Nb-50Zr (50Zr)	28	48	-	balance
Ti-27Nb-39Zr (39Zr)	38	28	-	balance
Ti-20Nb-30Zr-13Ta (30Zr)	21	29	13	balance

Table 2. Values of elastic modulus E (GPa), Vickers Microhardness (HV), Average Grain Size (μm) and Deformation (%RA) for all alloys in AC, HR, both (BC) conditions and for Ti-40Nb[33].

	50Zr	39Zr	30Zr	Ti-40Nb
Elastic Modulus (GPa)	77 (AC) ± 2	91 (AC) ± 2	83 (AC) ± 2	75 (AC)
	41 (HR) ± 1	70 (HR) ± 3	72 (HR) ± 2	69 (HR)
Vickers Microhardness (HV)	245 (AC) ± 22	228 (AC) ± 16	247 (AC) ± 20	226 (AC)
	237 (HR) ± 17	227 (HR) ± 13	233 (HR) ± 17	181 (HR)
Average Grain Size (μm)	119 (HR) ± 21	102 (HR) ± 16	96 (HR) ± 11	384 (AC)
				189 (HR)
Deformation (%RA)	57 (HR)	50 (HR)	54 (HR)	58 (HR)
Bcc - Lattice parameter (Å)	3.4271 ± 0.0015	3.3357 ± 0.0013	3.3152 ± 0.0031	---

Table 2 presents the data regarding the elastic modulus (GPa), Vickers microhardness (HV), average grain size, strain (%RA), and lattice parameter (a, Å) for all alloys in AC and HR conditions.

It was not observed that a significant variation in the hardness values if compared the condition AC with the RH. Despite the formation of the α", which has a lower hardness even than the β phase, the hardness remained practically unchanged because of strain hardening[27,30,32].

It is possible to notice a tendency to decrease the elastic modulus with the decrease of the lattice parameter. Furthermore, when comparing the AC condition with the HR condition, a reduction in the elastic modulus of 46% for the 50Zr alloy, 23% for the 39Zr, and 13% for the 30Zr alloy is observed. Thus, reaffirming that the hot-rolling process is an efficient route in optimizing β titanium alloys for biomedical applications. In addition, this result suggests that Zr may indeed influence the suppression of the formation of the omega phase since the 40Zr alloy showed the most significant reduction in the value of the elastic modulus and it is the one with the highest Zr content, approximately 48% (wt. %).

Figure 3 provides a graphic representation of the alloys studied here for the elastic modulus and the lattice parameter under AC and HR conditions.

When comparing the 50Zr alloy in this work with the Ti-40Nb alloy, it is possible to notice that adding Zr decreased the elastic modulus[32]. Since the two alloys have a very similar Nb weight percentage, for 50Zr with a percentage of reduction in the area (%RA) of 57%, it was determined that an elastic modulus of 41 GPa, while for Ti-40Nb has an elastic modulus of 69 GPa for %RA = 68%[32]. This is because Zr may be suppressing the formation of the omega phase, responsible for the increase in hardness and elastic modulus, the increase in the lattice parameter due to the addition of this element, and the reduction of the lower limit of e/a, which adjusts the atomic structure and elastic constants[12,43-47].

A direct relationship between the elastic modulus and the lattice parameters of the β phase is observed; increasing

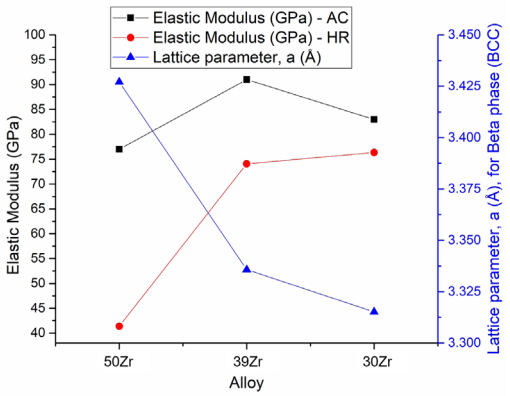

Figure 3. Variation of Elastic Modulus (GPa) and lattice parameter, a (Å), for β (BCC) for all alloys in the as-cast and hot-rolled conditions.

the value of the lattice parameter of the β phase decreased the elastic modulus of the 50Zr, 39Zr, and 30Zr alloys due to the decrease of the atomic strength of the β structure. Kuroda et al.[48] produced alloys of the Ti-25Ta-Zr system (Zr = 0, 10, 20, 30, and 40 in weight) and analyzed the changes in the lattice parameters of the α and β phases under the influence of the hot rolling process (1000 °C); in their results, it was observed that the hot rolling process dilates the HCP and BCC structures of titanium alloys, where higher values of alpha and β lattice parameters result in alloys with low values of elastic modulus. Thus, as seen by Kuroda, hot rolling decreased the elastic modulus of the 50Zr, 39Zr, and 30Zr alloys due to the dilation of the β lattice parameter.

In addition, as seen previously, the 50Zr alloy has a higher Mo_{eq} value (Mo_{eq} = 13.9) than the other alloys. Because of this, the 50Zr alloy has a lower elastic modulus among the alloys produced in this work. β-type Ti alloys tend to have a low elastic modulus.

4. Conclusions

The results lead to the following conclusions:

- The greater the Zr content, the higher the lattice parameter of bcc β phase, and the lower the elastic modulus of the β Ti-Nb-Zr(-Ta) multiprincipal alloys;
- The hot-rolling thermomechanical processing led to the formation of stress-induced martensite α″ (SIM) for β Ti-Nb-Zr(-Ta) alloys and consequent decreasing of elastic modulus, optimizing mechanical biocompatibility, reaching the best value of 41 GPa for Ti-30Nb-50Zr alloy.
- The decreasing of microhardness and the elastic modulus was due to the increase of the volumetric fraction of the martensite α″ (SIM) formed as a consequence of the deformation and, consequently, dynamic recrystallization;
- Hot rolling processing was confirmed to be a helpful route in order to reduce the elastic modulus for β-Ti multiprincipal alloys and opens perspectives of its application as metallic biomaterials.

5. Acknowledgments

This study was financed in part by the Coordenação de Aperfeiçoamento de Pessoal de Nível Superior - Brasil (CAPES) - Finance Code 001. The authors would like to thank Brazilian agencies CNPq Universal Project #422015/2018-0 (C.R.M.A.). To CAPES - Coordenação de Aperfeiçoamento de Pessoal de Nível Superior for the financial support to carry out this work with a grant process nº 88887.371759/2019-00 (R.F.M.S.). To FAPESP - Fundação de Amparo à Pesquisa do Estado de São Paulo for the financial support to carry out this work with "Projeto Temático" nº 2018/18293-8, Post-Doctoral Grant nº 2019/26517-6 (P.A.B.K.) and Scientific Initiation Grant nº 2020/12431-0 (C.N.R.)

6. References

1. United Nations. Department of Economic and Social Afairs. World population prospects 2019. New York; 2019.
2. Schwartz AM, Farley KX, Guild GN, Bradbury TL Jr. Projections and epidemiology of revision hip and knee arthroplasty in the United States to 2030. J Arthroplasty. 2020;35(6):S79-85. http://dx.doi.org/10.1016/j.arth.2020.02.030.
3. Kurtz S, Ong K, Lau E, Mowat F, Halpern M. Projections of primary and revision hip and knee arthroplasty in the United States from 2005 to 2030. J Bone Joint Surg Am. 2007;89(4):780-5. http://dx.doi.org/10.2106/00004623-200704000-00012.
4. Geetha M, Singh AK, Asokamani R, Gogia AK. Ti based biomaterials, the ultimate choice for orthopaedic implants: a review. Prog Mater Sci. 2009;54(3):397-425. http://dx.doi.org/10.1016/j.pmatsci.2008.06.004.
5. Basketter DA, Briatico-Vangosa G, Kaestner W, Lally C, Bontinck WJ. Nickel, cobalt and chromium in consumer products: a role in allergic contact dermatitis? Contact Dermat. 1993;28(1):15-25. http://dx.doi.org/10.1111/j.1600-0536.1993.tb03318.x.
6. Eisenbarth E, Velten D, Müller M, Thull R, Breme J. Biocompatibility of β-stabilizing elements of titanium alloys. Biomaterials. 2004;25(26):5705-13.
7. Landsberg JP, McDonald B, Watt F. Absence of aluminium in neuritic plaque cores in Alzheimer's disease. Nature. 1992;360(6399):65-8.
8. Yılmaz E, Gökçe A, Findik F, Özkan Gülsoy H. Characterization of biomedical Ti-16Nb-(0–4)Sn alloys produced by Powder Injection Molding. Vacuum. 2017;142:164-74.
9. Frost HM. Wolff's law and bone's structural adaptations to mechanical usage: an overview for clinicians. Angle Orthod. 1994;64:174-88.
10. Niinomi M, Nakai M. Titanium-based biomaterials for preventing stress shielding between implant devices and bone. Int J Biomater. 2011;2011:1-10.
11. Abdel-Hady Gepreel M, Niinomi M. Biocompatibility of Ti-alloys for long-term implantation. J Mech Behav Biomed Mater. 2013;20:407-15.
12. Yılmaz E, Gökçe A, Findik F, Gulsoy HÖ. Assessment of Ti–16Nb–xZr alloys produced via PIM for implant applications. J Therm Anal Calorim. 2018;134(1):7-14.
13. Yılmaz E, Kabataş F, Gökçe A, Fındık F. Production and characterization of a bone-like porous Ti/Ti-hydroxyapatite functionally graded material. J Mater Eng Perform. 2020;29(10):6455-67.
14. Bahl S, Suwas S, Chatterjee K. Comprehensive review on alloy design, processing, and performance of β Titanium alloys as biomedical materials. Int Mater Rev. 2021;66(2):114-39.
15. Ridzwan MIZ, Shuib S, Hassan AY, Shokri AA, Mohamad Ib MN. Problem of stress shielding and improvement to the hip implant designs: a review. J Med Sci. 2007;7(3):460-7.
16. Chaves JAM, Santos RFM, Ricci VP, Rodrigues AG, Afonso CRM. An exploratory study of TiO_2-based multicomponent nanotubes on TiFeNbSn ultrafine eutectic alloy. Surf Coat Tech. 2021;407:126765.
17. Ricci VP, Santos RFM, Asato GH, Roche V, Jorge AM, Afonso CRM. Assessment of anodization conditions and annealing temperature on the microstructure, elastic modulus, and wettability of β-Ti40Nb alloy. Thin Solid Films. 2021;737:138949.
18. Kuroda PAB, Quadros FF, Nascimento MV, Grandini CR. Development and characterization of new Ti-25Ta-Zr alloys for biomedical applications. Mater Sci Forum. 2021;1016:137-44.
19. Liang S. Review of the design of titanium alloys with low elastic modulus as implant materials. Adv Eng Mater. 2020;22(11):2000555.
20. Yılmaz E, Gökçe A, Findik F, Gulsoy HO, İyibilgin O. Mechanical properties and electrochemical behavior of porous Ti-Nb biomaterials. J Mech Behav Biomed Mater. 2018;87:59-67.
21. Kuroda PAB, Silva LM, Sousa KSJ, Donato TAG, Grandini CR. Preparation, structural, microstructural, mechanical, and cytotoxic characterization of Ti-15Nb alloy for biomedical applications. Artif Organs. 2020;44(8):811-7.
22. Bönisch M, Calin M, Giebeler L, Helth A, Gebert A, Skrotzki W, et al. Composition-dependent magnitude of atomic shuffles in Ti–Nb martensites. J Appl Cryst. 2014;47(4):1374-9.
23. Yi R, Liu H, Yi D, Wan W, Wang B, Jiang Y, et al. Precipitation hardening and microstructure evolution of the Ti–7Nb–10Mo alloy during aging. Mater Sci Eng C. 2016;63:577-86.
24. Afonso CRM, Amigó A, Stolyarov V, Gunderov D, Amigó V. From porous to dense nanostructured β-Ti alloys through high-pressure torsion. Sci Rep. 2017;7(1):13618.
25. Gonzalez ED, Afonso CRM, Nascente PAP. Influence of Nb content on the structure, morphology, nanostructure, and properties of titanium-niobium magnetron sputter deposited coatings for biomedical applications. Surf Coat Tech. 2017;326:424-8.
26. Afonso CRM, Aleixo GT, Ramirez AJ, Caram R. Influence of cooling rate on microstructure of Ti–Nb alloy for orthopedic implants. Mater Sci Eng C. 2007;27(4):908-13.
27. Dobromyslov AV, Elkin VA. β→α″ and β→ω transformations in Ti-Os alloys. Metall Mater Trans, A Phys Metall Mater Sci. 1999;30(1):231-3.
28. Ho W, Ju CP, Chern Lin JH. Structure and properties of cast binary Ti–Mo alloys. Biomaterials. 1999;20(22):2115-22.

29. Nag S. Influence of beta instabilities on the early stages of nucleation and growth of alpha in beta titanium alloys. Ohio: The Ohio State University; 2008.
30. Ohmori Y, Ogo T, Nakai K, Kobayashi S. Effects of ω-phase precipitation on β→α, α″ transformations in a metastable β titanium alloy. Mater Sci Eng A. 2001;312(1-2):182-8.
31. Sheremetyev V, Kudryashova A, Cheverikin V, Korotitskiy A, Galkin S, Prokoshkin S, et al. Hot radial shear rolling and rotary forging of metastable beta Ti-18Zr-14Nb (at. %) alloy for bone implants: microstructure, texture and functional properties. J Alloys Compd. 2019;800:320-6.
32. Geng F, Niinomi M, Nakai M. Observation of yielding and strain hardening in a titanium alloy having high oxygen content. Mater Sci Eng A. 2011;528(16-17):5435-45.
33. Santos RFM, Ricci VP, Afonso CRM. Influence of swaging on microstructure, elastic modulus and vickers microhardness of β Ti-40Nb alloy for implants. J Mater Eng Perform. 2021;30(5):3363-9.
34. Chen Y, Li J, Tang B, Kou H, Xue X, Cui Y. Texture evolution and dynamic recrystallization in a beta titanium alloy during hot-rolling process. J Alloys Compd. 2015;618:146-52.
35. Alkhazraji H, El-Danaf E, Wollmann M, Wagner L. Enhanced fatigue strength of commercially pure Ti processed by rotary swaging. Adv Mater Sci Eng. 2015;2015:1-12.
36. Senopati G, Sutowo C. Effect of hot rolling on structure and hardness of α/β Ti-6Al-6Nb alloy for orthopedic application. AIP Conf Proc. 2023;2630:040002.
37. Mehjabeen A, Xu W, Qiu D, Qian M. Redefining the β-phase stability in Ti-Nb-Zr alloys for alloy design and microstructural prediction. J Miner Met Mater Soc. 2018;70(10):2254-9.
38. Callister WD, Rethwish DG. Materials science and engineering: an introduction. Hoboken: Wiley-VCH; 2014.
39. ASTM: American Society for Testing and Materials. ASTM E1876-15: Standard test method for dynamic Young's modulus, shear modulus, and Poisson's ratio by impulse excitation of vibration. West Conshohocken: ASTM; 2015.
40. ASTM: American Society for Testing and Materials. ASTM E384-17: standard method for microindentation hardness of materials. West Conshohocken: ASTM; 2017.
41. Blackburn MJ, Williams JC. Phase transformations in Ti--Mo and Ti--V alloys. Trans Metall Soc AIME. 1968;242:2461-9.
42. Dey GK, Tewari R, Banerjee S, Jyoti G, Gupta SC, Joshi KD, et al. Formation of a shock deformation induced ω phase in Zr 20 Nb alloy. Acta Mater. 2004;52(18):5243-54.
43. Min XH, Emura S, Zhang L, Tsuzaki K. Effect of Fe and Zr additions on ω phase formation in β-type Ti–Mo alloys. Mater Sci Eng A. 2008;497(1-2):74-8.
44. Ferrandini PL, Cardoso FF, Souza SA, Afonso CR, Caram R. Aging response of the Ti–35Nb–7Zr–5Ta and Ti–35Nb–7Ta alloys. J Alloys Compd. 2007;433(1-2):207-10.
45. Li Q, Niinomi M, Nakai M, Cui Z, Zhu S, Yang X. Effect of Zr on super-elasticity and mechanical properties of Ti–24at% Nb–(0, 2, 4)at% Zr alloy subjected to aging treatment. Mater Sci Eng A. 2012;536:197-206.
46. Kim JI, Kim HY, Inamura T, Hosoda H, Miyazaki S. Shape memory characteristics of Ti–22Nb–(2–8)Zr(at.%) biomedical alloys. Mater Sci Eng A. 2005;403(1-2):334-9.
47. Kim KM, Kim HY, Miyazaki S. Effect of Zr content on phase stability, deformation behavior, and young's modulus in Ti–Nb–Zr alloys. Materials. 2020;13(2):476.
48. Kuroda PAB, Grandini CR, Afonso CRM. Structural characterization of the hot-rolled Ti-25Ta-xZr alloys by Rietveld method. Mater Res. 2023;26(Suppl 1):e20220559.